

ORIGINAL RESEARCH

Open Access

Empirical model assessment of commercial aircraft emissions according to flight phases

Enis T Turgut^{1*}, Oznur Usanmaz² and Marc A Rosen³

Abstract

The quantities of common emissions are investigated for a specific type of commercial aircraft. Actual flight data and International Civil Aviation Organization emission data are used. All flight phases are considered, including landing and takeoff phases. The investigation is carried out for the domestic flights only and considers relevant parameters, such as engine type, flight phase, and ground or air operation of the flight. The findings suggest that the quantities of emissions of unburned hydrocarbon (HC) and carbon monoxide (CO) during the descent phase can exceed those for the taxi phases and the idle operation of the engines, depending on the approach procedure. The main source of nitrogen oxide (NO_x) is usually the climb phase, while the mean total flight emissions are calculated as 6 to 8 kg of HC, 60 to 75 kg of CO, and 28 to 31 kg of NO_x. The effect of the duration of taxi phase on the production of HC and CO emissions is also discussed.

Keywords: Aircraft emission, Environment, Turbofan engine, Flight data records

Background

Since the advent of turbofan engines in 1960s, there has been an increase in the commercial flights and, correspondingly, air traffic movement in the vicinity of airports. The increase in air traffic has led to some problems, e.g., noise and environmental impact through emissions. Noise is perceived easily and can be monitored and regulated. Regulations related to aircraft emissions began to be put in place by the Environmental Protection Agency (EPA) in 1974, starting with smoke monitoring and followed by regulations for hydrocarbon emissions (1984), nitrogen oxide (NO_x) and carbon monoxide (CO) (1997), and further controls for NO_x (2005).

In the last 20 years, much effort has been expended to improve understanding and reduction of the environmental impact of aircraft by such organizations as the Federal Aviation Administration, National Aeronautics and Space Administration, European Organisation for the Safety of Air Navigation, International Civil Aviation Organization (ICAO), International Air Transport Association, and Civil Air Navigation Services Organisation. Databases involving fuel consumption and emissions of

NO_x, CO, and hydrocarbon (HC) for the scheduled civil aviation were developed in 1992 [1] and 1996 [2]. Studies have included investigations of aircraft NO_x emissions within the ANCAT/EC project [3], analyses of emissions resulting from civil and military aviation within the project of Global Aviation Emissions Inventories for 2002 and 2025 (AERO2K) [4], and theoretical aircraft fuel consumption and emission modeling within the project of System for Assessing Aviation's Global Emissions [5].

Moreover, aircraft emissions have become an important issue not only for aviation authorities but also environmental scientists and the public. According to the EPA, aircraft engines were responsible for 2% of the total US mobile emission sources in 1997. However, it is reported that aircraft can contribute up to 4% of emissions in the vicinity of airports [6]. In addition, difficulties in measuring the altitude of flight emissions have motivated numerous studies focusing on the generation and identification of emissions in the vicinity of the airports such as Atlanta, Heathrow, New York, Los Angeles, Zurich, and Copenhagen [7-13].

Nevertheless, improved information is needed on aircraft emissions according to flight phases. The objective of this study is to improve understanding on common emissions (HC, CO, and NO_x) resulting from aircraft, based on the ICAO databank [14]. This databank includes exhaust

* Correspondence: etturgut@anadolu.edu.tr

¹Department of Airframe and Powerplant Maintenance, Faculty of Aeronautics and Space Sciences, Anadolu University, Eskisehir 26470, Turkey
Full list of author information is available at the end of the article

emissions and fuel flow rates for currently used turbofan engines during landing and takeoff (LTO) phases. The investigation is carried out in such a way that the actual flight data are considered. In order to perform this task, a novel method is developed, in which interpolation and extrapolation of the relationship between the fuel flow and the emission indices data of specific types of engine are provided. Data are obtained from flights of ten randomly selected B737-800 (hereafter B738) commercial aircraft. Two types of turbofan engines are used in these aircraft: CFM56-7B26 and CFM56-7B26/3.

Analysis setup

The most frequently used domestic routes, aircraft types, and the engine types are considered for the data selection. For this purpose, ten randomly selected B738 commercial aircraft are used. Five of them are for flights between the Antalya International (AYT) and Sabiha Gokcen International (SAW) airports, and five are for flights between the Izmir Adnan Menderes International (ADB) and the SAW airports. The SAW airport is the arrival airport for each group. The airports are defined in Table 1. All flights occurred in 2009.

The route selections relate to the frequency of flights to SAW. In 2009, for domestic flights, the two most frequent arrivals to SAW are from ADB and AYT, with 2,956 and 2,684 total arrivals, respectively. For B738 aircraft only, the numbers of arrivals reduce to 1,540 for AYT and 1,134 for ADB. Of the total arrivals to SAW with B738 aircraft, flights from AYT and ADB account for 15% and 11%, respectively. Other arrival percentages are shown in Figure 1.

According to the traffic statistics of the SAW airport in 2009, the most used aircraft type is the B738. Taking into account all aircraft traffic to or from the SAW airport (including international flights), those utilizing the B738 aircraft account for the largest proportion at 47%. Therefore, ten randomly selected B738 flights are evaluated here, all from 2009. Actual flight data of these flights are obtained from Pegasus Airlines, an international airline based in Turkey. Considered in the analysis are aircraft flight parameters such as aircraft altitude, ground speed and weight, as well as engine parameters such as fuel flow rate,

rotation speeds of the low pressure system (N1) and the high pressure system (N2) on percentage bases, and exhaust gas temperature (EGT).

With respect to engines, six of the assessed flights were powered by CFM56-7B26 (hereafter 7B26) engines, while the remaining four were powered by CFM56-7B26/3 (hereafter 7B26/3) turbofan engines. Moreover, for the flights of each route, three 7B26 and two 7B26/3 engines are utilized.

Methods

In the ICAO emission databank, there are 17 different models of the CFM56-7B series engine, which can be tabulated according to bypass ratio, overall pressure ratio, and thrust parameters (see Table 2). The engine family can be classified into three groups: CFM56-7BX (single annular combustion), CFM56-7BX/2 (double annular combustion), and CFM56-7BX/3 (improved emission single annular combustion), where *X* denotes model numbers such as 18, 20, 22, 24, 26, and 27 [15]. The classification is mainly based on the combustion chamber design.

As can be seen from Table 2, there is an inverse relationship between the model number (which increases moving down the list in Table 2) and the bypass ratio, and a direct relationship between the model number and the pressure ratio and the thrust in each group. This pattern is valid for all three engine groups.

The ICAO emission database has a disadvantage in that its emission indices are obtained only for limited fuel flow rates. For instance, a single fuel flow rate is accepted for the entire flight phase. This prevents a precise identification of the emissions generated from commercial aircraft since the fuel flow rate is not constant. To address this problem here, the approach used in this study is developed based on linear and polynomial extrapolation and interpolation for three types of emissions: HC, CO, and NO_x. Nonetheless, it is noted that emission production mechanisms generally are not simple. In this regard, equivalence ratio, combustion temperature, and compressor pressure ratio, all of which vary with engine power, or the ambient conditions might significantly influence the emissions, and numerous studies of these influences have been reported [7,8,16-18].

Table 1 Airport information

Aerodrome location indicator and name	ARP geographical coordinates	Distance to SAW (km)	Aircraft movement ^a
SAW - Istanbul Sabiha Gokcen International	40°53'54"N, 29°18'33"E	-	63,749
ADB - Izmir Adnan Menderes International	38°17'21"N, 27°09'18"E	344	54,197
AYT - Antalya International	36°54'01"N, 30°47'34"E	462	127,236

ARP aerodrome reference point. ^aAircraft movement is defined at [http://icaodata.com/Terms.aspx# AircraftMovement%28airports%29](http://icaodata.com/Terms.aspx#AircraftMovement%28airports%29) as 'an aircraft take-off or landing at an airport. For airport traffic purposes one arrival and one departure is counted as two movements.' The airport movement statistics for 2009 are retrieved from <http://dhmi.gov.tr/istatistik.aspx>.

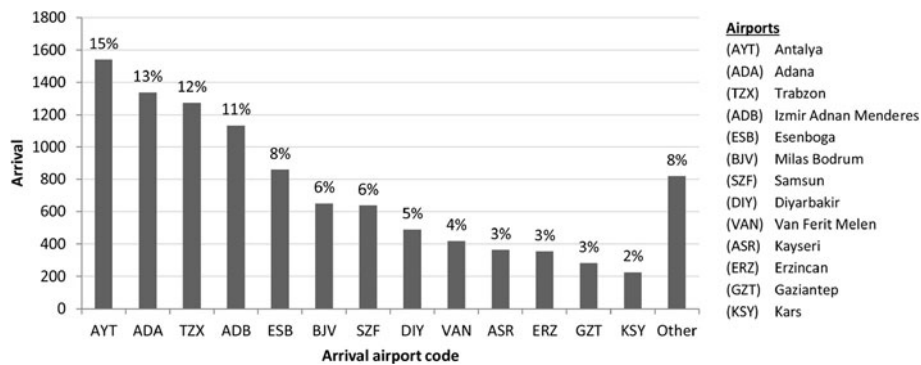


Figure 1 Breakdown of domestic arrivals to Sabiha Gokcen International (SAW) airport of B738 aircraft for 2009. The 'other' category denotes flights from the other 12 domestic airports, which each have an arrival number of less than 200.

In the ICAO emission database, fuel flow rates and emission indices are given by engine model for the following flight phases: takeoff, climb, approach, and idle. Excluding the 7BX/2 series, it is noted that there are 24 (6×4) fuel flow rate and emission indices observations for either 7BX or 7BX/3 series engines. These 24 data groups generate the observation domain for each engine group, which is used for establishing the relationships between the fuel flow and the specific emission indices. Since six of the flights are performed with the aircraft having a 7BX series engine and four of the flights are performed with the aircraft having a 7BX/3 series engine, two engine models are considered here. Therefore, the results are different from those in which a single engine type is considered.

Table 2 Specific performance parameters of CFM56-7B series engines (modified from [14])

Engine model	Bypass ratio	Pressure ratio	Thrust (kN)
CFM56-7B18	5.5	21.6	86.7
CFM56-7B20	5.4	22.6	91.6
CFM56-7B22	5.3	24.4	101.0
CFM56-7B24	5.2	25.8	107.7
<i>CFM56-7B26</i>	<i>5.1</i>	<i>27.6</i>	<i>117.0</i>
CFM56-7B27	5.0	28.6	121.4
CFM56-7B20/2	5.4	22.8	91.6
CFM56-7B22/2	5.3	24.6	101.0
CFM56-7B24/2	5.2	25.9	107.7
CFM56-7B26/2	5.1	27.8	117.0
CFM56-7B27/2	5.0	28.8	121.4
CFM56-7B18/3	5.5	21.4	86.7
CFM56-7B20/3	5.5	22.4	91.6
CFM56-7B22/3	5.3	24.2	101.0
CFM56-7B24/3	5.3	25.6	107.6
<i>CFM56-7B26/3</i>	<i>5.1</i>	<i>27.7</i>	<i>117.0</i>
CFM56-7B27/3	5.1	29.0	121.4

Italic font indicates the sample engines.

The variation of common emission indices with fuel flow rate indicates that linear relationships are present for certain fuel flow fragments, where fuel flow fragments are the fuel flow rate regions for a given flight phase for all of the engines. For instance, the given fuel flow rates for the climb phases of all the engine models constitute a fuel flow region, while there are other specific fuel flow ranges for the other three flight phases: takeoff, approach, and landing. In other words, there is specific fuel flow region for each flight phase for the engines of each group. For these regions, the relationship between the emission indices and the fuel flow rates can be straightforwardly identified. However, for fuel flow rates outside the specified regions, particularly between the two regions, the approach based on the aforementioned relationship can lead to incorrect results. Therefore, one needs additional methods which can be obtained utilizing the sequential regions. For instance, if the overall fuel flow ranges are divided into three parts (highest, medium, and lowest regions indicating the amount of fuel flow), then the region between the highest and medium fuel flow rates and also between the medium and the lowest fuel flow rates can be described by additional relationships. The required model descriptions are presented in the following section.

Results and discussion

The relationships are developed for two sections, representing both engine series, and given in Tables 3 and 4. The fuel flow range is also given in these tables. The coefficients of determination (R^2) for the regression models are given in the last columns of Tables 3 and 4. All of the regression models exhibit high coefficients of determination, mostly over 0.960 (with the exceptions of 0.904 and 0.910, which relate to the fuel flow range of CO emissions). This means that these models explain more than 96.0% of the variation in emission index when compared to the total variation.

The relationships between the emission index (EI) for common emissions and the fuel flow rate (ff) which are

Table 3 Model emission indices for CFM56-7BX (flights 1, 3, 4, and 6 to 8)

Emission index (EI) (g)	ff range (kg s ⁻¹)	Model ^a	R ²
EI (HC)	ff ≥ 0.260	0.1	0.978
	0.260 > ff > 0.116	0.0029 × (ff) ^{-2.988}	0.979
	0.09 ≤ ff ≤ 0.116	-92.07 × (ff) + 12.34	NA ^b
EI (CO)	ff ≥ 0.714	9.10 × (ff) ³ - 30.46 × (ff) ² + 32.52 × (ff) - 10.61	0.975
	0.714 > ff > 0.349	0.42 × (ff) ^{-1.446}	0.904
	0.349 ≥ ff ≥ 0.260	-24.64 × (ff) + 9.95	0.995
	0.260 > ff > 0.116	0.17 × (ff) ^{-2.194}	0.995
	ff ≤ 0.116	-536.95 × (ff) + 79.89	0.981
EI (NO _x)	ff > 0	20.29 × (ff) + 2.83	0.989

ff fuel flow rate; NA not available. ^aCoefficients in the models are rounded to two decimals in most cases. ^bEI of HC for this range is given in the ICAO database as a constant value of 0.1 g HC/kg of fuel.

both obtained from the ICAO database are shown in Figures 2, 3, 4 and 5. Regarding the HC emissions for the two types of engines considered, it can be seen that the EI for HC emissions can be divided into three parts for 7BX engines: 0.09 to 0.116 kg/s (lower ff), 0.116 to 0.260 kg/s (moderate ff), and above 0.260 kg/s (higher ff). On the other hand, there are five parts for HC emissions for 7BX/3 engines. However, if we focus on the lower ff range, such as below 0.110 kg/s, it can be seen that the EI for HC emissions of 7BX engines is low compared to 7BX/3 engines, while between the top and bottom limits at this part (0.09 to 0.110 kg/s), the slope of the curve for 7BX/3 engines is steeper (see Figures 2a and 3a). Generally, it can be noted that the EI for HC

emissions of 7BX/3 engines is greater than for 7BX engines. In order to understand the effect of these small values, note that the idle ff value of these types of engines is in the order of 0.070 kg/s (no aircraft movement) and 0.097 kg/s (during taxi) per engine (although values can differ due to other factors such as the mass of aircraft or ambient temperature).

Similar behavior is exhibited by the EI for CO emissions. The EI for CO emissions of 7BX/3 is usually higher than for 7BX engines, except those for higher ff values (above 0.714 kg/s). Also, in this ff segment, the relation between EI to ff is significantly changed (see Figure 4).

As seen in Figures 2, 3 and 4, there can be interruptions between certain data values. Reasonable ff values in the interrupted region can be estimated by considering front and rear regions such as done in Figure 2b. Therefore, since there is no ICAO information regarding the EI for corresponding ff values in these regions, the precision of the predictions for these regions is likely lower. Nonetheless, estimates for these regions are often useful.

Lastly, regarding the EI for NO_x emissions, it is seen in Figure 4 that the 7BX/3 engines produce less emissions per kilogram of fuel. This result is expected, since these engines produce less NO_x due to combustor upgrades (recall that it was found earlier that EIs for HC and CO emissions are higher compared to other types of engines). Furthermore, a higher ff leads to higher NO_x emissions, indicating a direct relationship.

Considering overall ff ranges, it appears from the ICAO results that the relationships between ff values and HC and CO emissions are nonlinear (which for the HC case is also stressed in [18] and elsewhere), while it is linear for the EI for NO_x emissions.

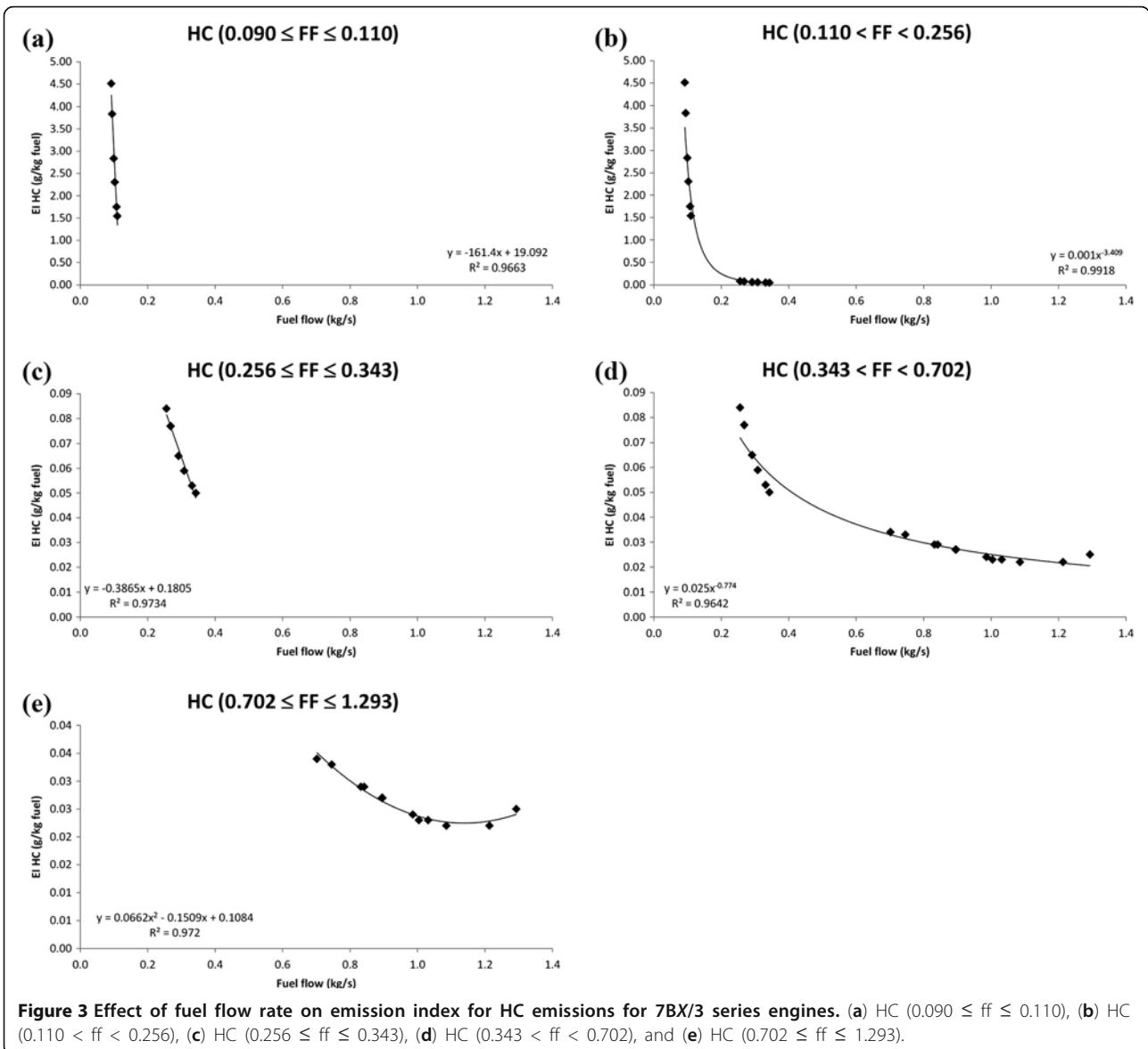
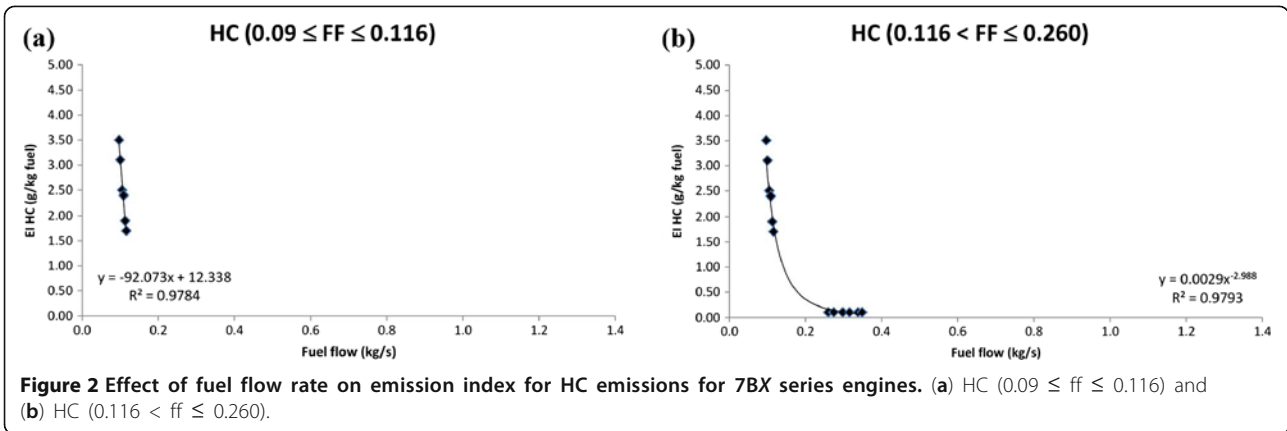
In Figures 6 and 7, the variations of ff vs. flight phase and flight time are shown. It can be seen that the critical phases for HC and CO emissions are phases 1 and 2 as well as 9 to 14. Of these, phases 2 and 9 in particular produce more HC and CO emissions due to having high durations and less engine power. Regarding phase 9, controlling the production of these types of emissions might be possible by following different descent patterns leading to increased engine power; however, this action would increase NO_x emissions and also the fuel consumption. From a NO_x perspective, on the other hand, phases 3 to 7 appear to be more critical.

To identify the emissions of each flight, a detailed analysis is carried out in this section. Accordingly, the emissions are determined for each route due to the different distances between the departure and the arrival airports, and thereby the fuel consumptions. Each route involves five flights. As stated earlier, two of the five aircraft on each route use the CFM56-7B26/3 engine, while the other three use the CFM56/7B26. As shown in Table 2,

Table 4 Model emission indices for CFM56-7BX/3 (flights 2, 5, 9, and 10)

Emission index (EI) (g)	ff range (kg s ⁻¹)	Model ^a	R ²
EI (HC)	ff ≥ 0.702	0.07 × (ff) ² - 0.15 × (ff) + 0.11	0.972
	0.702 > ff > 0.343	0.03 × (ff) ^{-0.77}	0.964
	0.343 ≥ ff ≥ 0.256	-0.39 × (ff) + 0.18	0.973
	0.256 > ff > 0.110	0.001 × (ff) ^{-3.41}	0.992
	ff ≤ 0.110	-161.40 × (ff) + 19.09	0.966
EI (CO)	ff ≥ 0.702	1.56 × (ff) ² - 3.03 × (ff) + 1.63	0.972
	0.702 > ff > 0.343	0.18 × (ff) ^{-2.43}	0.910
	0.343 ≥ ff ≥ 0.256	-31.11 × (ff) + 13.37	0.991
	0.256 > ff > 0.110	0.32 × (ff) ^{-2.07}	0.999
	ff ≤ 0.110	-944.89 × (ff) + 132.56	0.985
EI (NO _x)	ff > 0	14.79 × (ff) + 3.04	0.984

^aCoefficients in the models are rounded to two decimals in most cases.



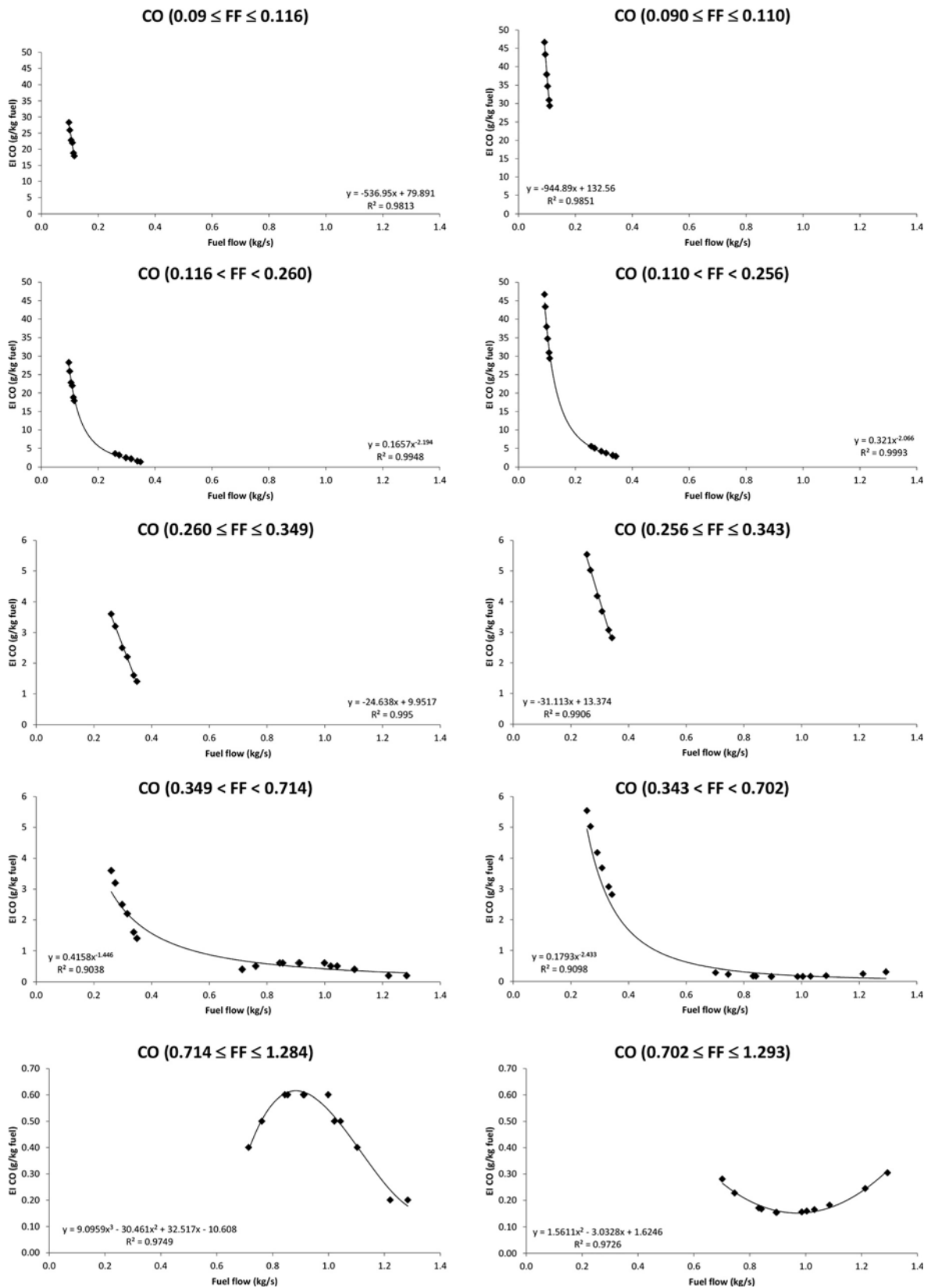
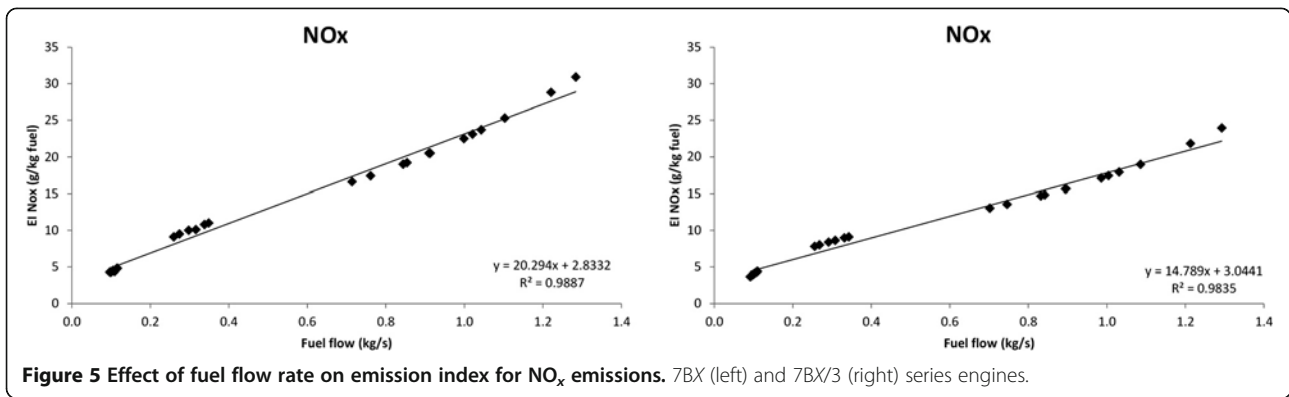


Figure 4 Effect of fuel flow rate on emission index for CO emissions. 7BX (left) and 7BX/3 (right) series engines.



the bypass ratio, the pressure ratio, and the thrust of these two kinds of engines are the same. Nonetheless, the combustion chamber designs differ, impacting the emission production mechanism. According to Brasseur et al., rich mixtures and the local flame extinctions in the combustion chamber are likely to induce CO and HC production, respectively [19]. This addresses the importance of the design of the primary zone of the combustion chambers, residence time of the flame, and the flame temperature [20,21]. Also, ambient temperature could affect the engine thermal efficiency and thereby certain emission types [18].

Consequently the following analyses are performed in the following subsections: 'Emission breakdown by flight phase' and 'Flight phase duration vs. amount of emissions.'

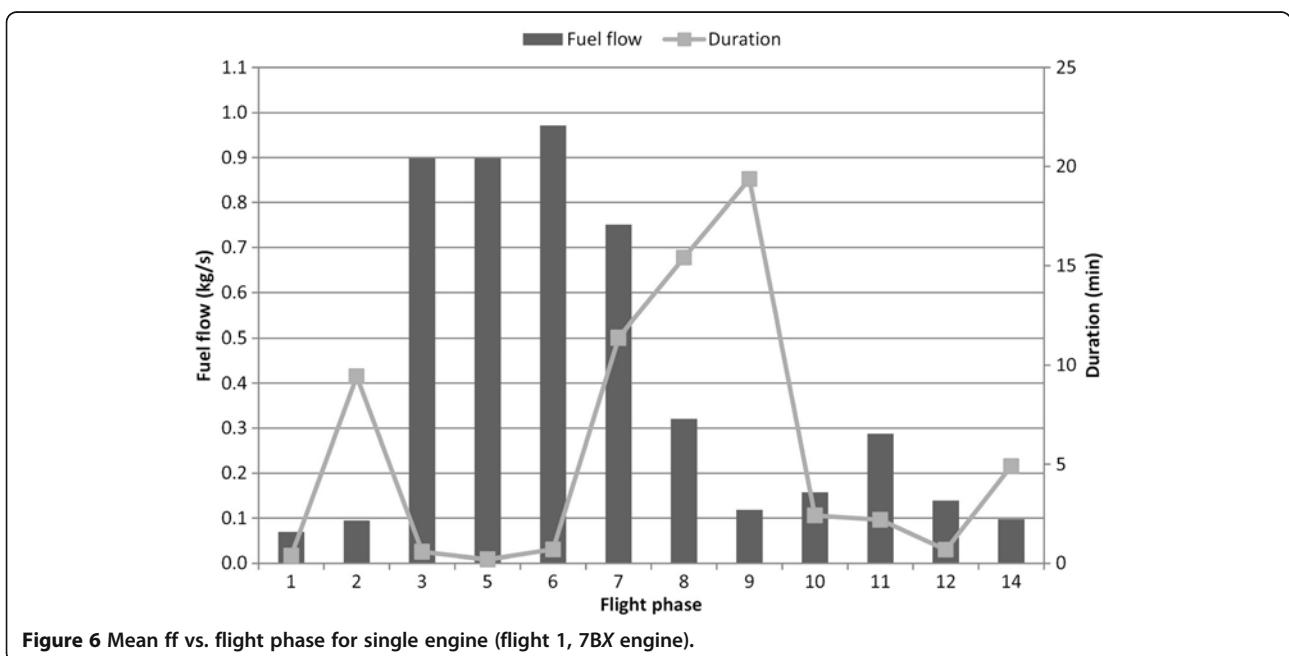
Emission breakdown by flight phase

In the ICAO database, emission indices are given for only four flight phases. Utilizing the models developed

in this study, one can obtain information related to other flight phases, such as cruise and taxi.

The duration of the flight phases are depicted in Figure 8. Since the flights are domestic and short range, the LTO phases constitute the larger part of the total flight duration. The duration of the phases can change significantly for international flights.

From the perspective of the flight phase where emission production takes place, it can be useful to know the breakdown of aircraft utilization on the ground and in the air. In this context, all flights are examined in terms of the utilization duration. The results indicate that the percentage of ground utilization of the aircraft ranges between 22% to 29% for AYT and 18% to 27% for ADB departures, respectively. The averages of ground utilization of the aircraft by route are around 25% and 22%, respectively. That is, almost one fourth of the operation duration takes place on the ground.



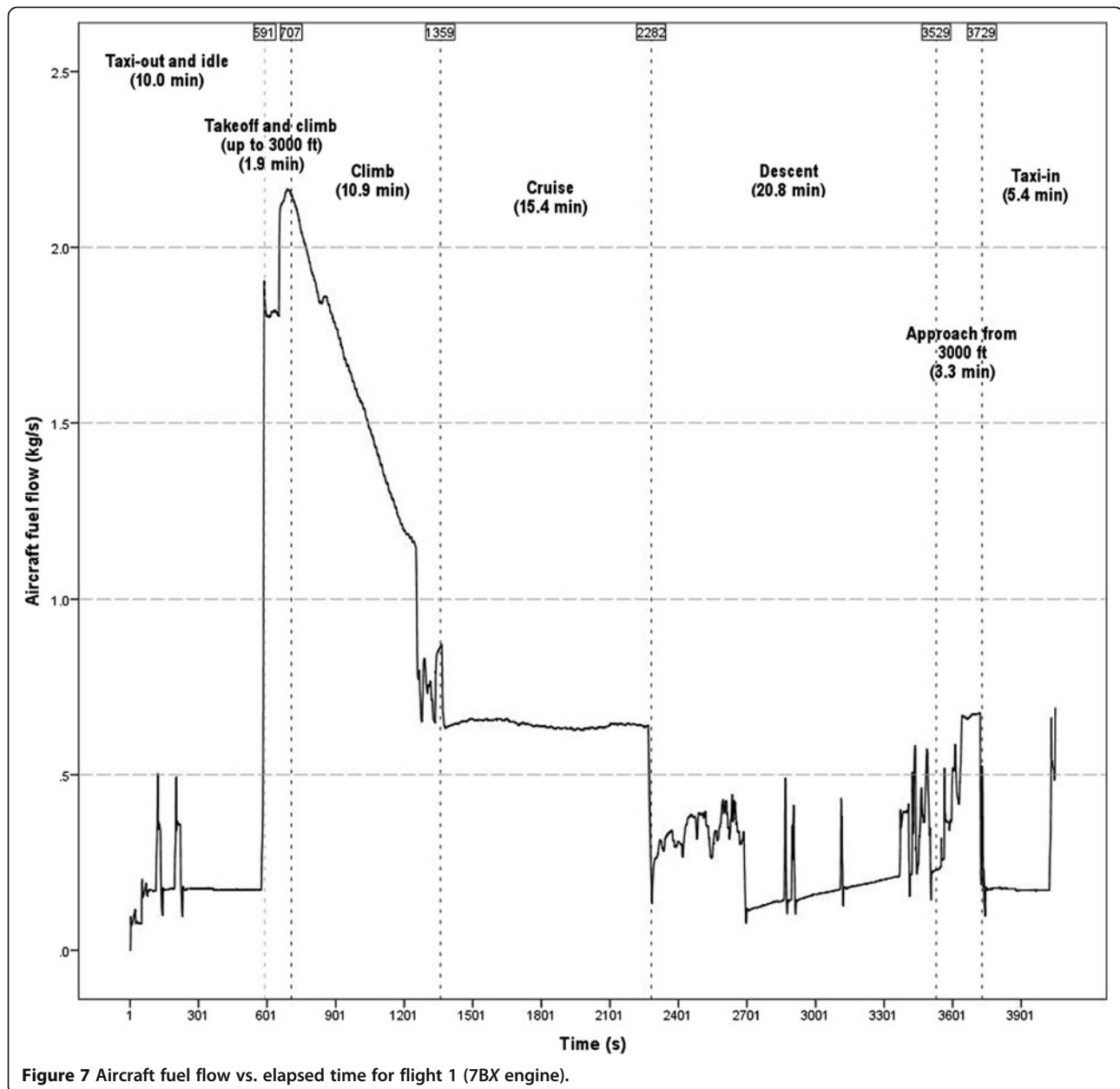


Figure 7 Aircraft fuel flow vs. elapsed time for flight 1 (7BX engine).

The breakdowns of the HC, CO, and NO_x emissions for the AYT-SAW route are shown in Figure 9a. It is seen that certain emission types produced at certain flight phases can vary greatly from those for the other phases. On the other hand, the same flight phase can exhibit a relatively lower amount of some kinds of emission types and a relatively higher amount of other types of emissions. Here, it is noted that the engine power setting and phase duration significantly affect emission quantities.

Due to incomplete combustion, the emissions of HC and CO for lower engine power settings are observed to be much greater than those for higher power settings

[2,12,22,23]. Therefore, such emissions obtained for flight phases such as taxi and descent are found to be higher than the phases such as takeoff and climb. This pattern is observed from the graphs in Figure 9. Accordingly, HC and CO emissions resulting from aircraft operation during taxi (P2 for taxi out and P14 for taxi in) and descent (P12), where the engine power setting is relatively low, are observed to be at higher levels. For instance, the HC emissions are calculated as 3.7 and 3.8 kg for the sum of P2 and P14, and P9, respectively. Since the phase duration can have a great effect on the emissions, the duration should be considered along with the amount of the emissions.

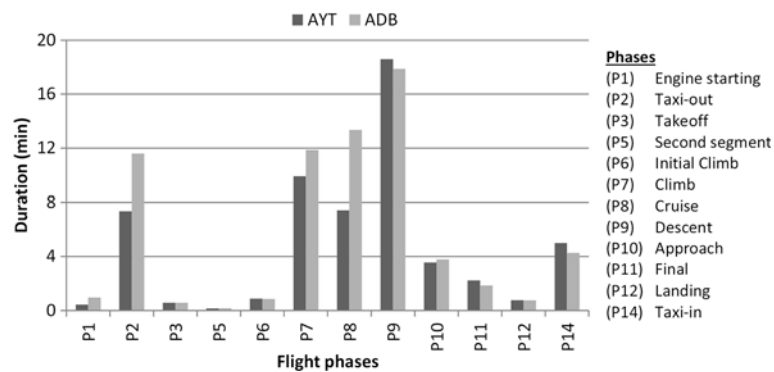


Figure 8 Durations of flight phases. The average total flight times are 67.9 and 56.8 min for AYT and ADB, respectively.

As can be seen from the graphs in Figure 9, for relatively lower power settings as for the idle and taxi (P2 and P14) phases, higher quantities of HC and CO emissions are observed, depending on the phase duration. For instance, the highest levels of HC emissions are observed for the phases of descent, taxi out, and taxi in, for which the corresponding durations are 18, 12, and 4 min. Considering the air quality in the vicinity of the airport (related to flight phases P1 to P3 and P12 to P14), it is found that 2.9 kg of HC is produced in AYT and 0.8 kg in SAW. Although the emission production mechanism during taxi in is not fundamentally different from that for taxi out, the difference in HC emissions results from the longer taxi duration at AYT. HC emissions are much lower for the other flight phases.

In the above discussions, the flight phases P3 (takeoff) and P12 (landing) are assumed to occur in the vicinity of the airport since the flight phases occur at a low height over the runway. For instance, the average heights for AYT-SAW routes are determined to be 19 m for P3 and 12 m for P12. As a result, the durations of the idle and taxi phases have significant effects on the quantities of HC emissions. For the above example, the longer ground operation duration (P1 to P3) at the departure airport AYT yields a higher HC emission (2.9 kg), while the shorter ground operation (P12 to P14) in the arrival airport SAW yields a lower HC emission (0.8 kg). Thus, for the high air traffic in busy airports, where aircraft often waits in taxi sequence or holding point for takeoff in long queues, or for airports with long taxi ways, there may be significant HC emissions in the vicinity of the airport.

The descent flight phase (P9) is the longest phase. In this phase, depending on the descent procedure, the power settings of the engine can be idle or at a value slightly higher than the idle. For instance, the N1 revolutions per minute (RPM) of the engine for the 9th flight is calculated at around 30% to 35% of the actual RPM at full speed, after 89% of the descent time has elapsed. During the same phase, the EGT values are concentrated

at 426°C to 429°C. By comparison, the distributions of the N1 RPM and the EGT values for the taxi phase are concentrated at around 18% to 24% and 470°C to 530°C, respectively. Although the lower power settings may lead to higher HC emissions, the net benefit can be positive due to reduced fuel consumption and amounts of other emissions, such as NO_x and carbon dioxide (CO₂).

The emission breakdown of CO by flight phase is similar to those for HC emissions. However, the mass of CO emissions can be an order of magnitude higher than that of HC emissions. As seen in Figure 9a, the highest CO emissions are observed for the flight phases of descent (34.0 kg), taxi in (25.3 kg), and taxi out (7.4 kg), which are similar to the case for HC emissions. CO emissions are found to be quite low for the remaining flight phases, for which power settings are relatively high.

The total HC and CO emissions for the AYT-SAW route are calculated as 8 and 76 kg, respectively. According to [2], approximately 70% of CO and HC releases are emitted below 9-km altitude. In this study, this range is further refined. Dividing the entire flight into the two categories as air and ground, it can be observed that almost half of the total emissions of both types are produced during ground operations, with flight phases of takeoff (P3) and landing (P12) included in ground operations. Considering two categories, the percentage of the average flight phase durations and fuel consumptions of the ground category for these five flights are determined to be 27% and 11%, respectively.

The highest levels of NO_x emissions are observed during the climb, cruise, and descent phases. The average NO_x emissions for the five flights is 31.3 kg, of which 16.0% is produced in ground operations, 34.6% in climb, 20.6% in cruise, and 15.9% in descent. Taxi in exhibits higher NO_x emissions than taxi out due to the longer phase duration.

The emissions and the fuel consumptions for the second route (ADB-SAW) are shown in Figure 9b. Although the duration of the flight phases differs from flights of

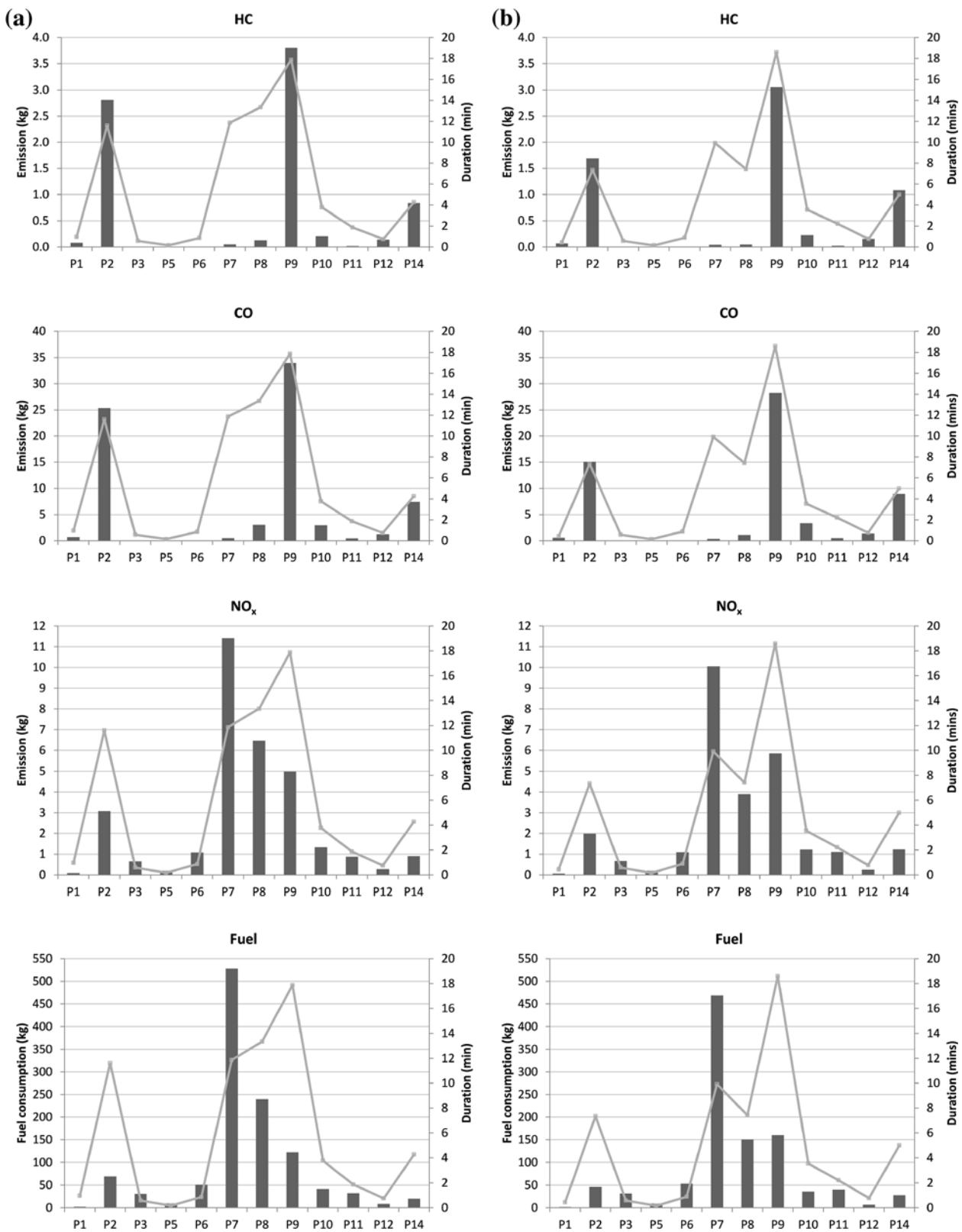


Figure 9 Emission breakdown by flight phase for (a) AYT and (b) ADB departures. The gray line in each graphic indicates the duration of the related phase.

the first route, the emission trends are similar to those for the first route, particularly for HC and CO. That is, the descent and the taxi phases exhibit the highest HC and CO emissions. Similarly, the highest HC and CO emissions are observed for the descent phase. Due to different route and fuel consumption values, the emissions are found to be lower than those for the previous route, as expected. However, the decrease in the emissions is not proportional to the decrease in the fuel consumptions. Accordingly, the average of the fuel consumption of ADB-SAW flights is 11% lower than the fuel consumption of AYT-SAW flights, while the HC and CO emissions are found to be 21% lower than those for the second route. However, the NO_x emissions are found to be 12% lower than the ADB-SAW flights. That is, there is a similar relationship between fuel flow and NO_x emissions, but the effect of fuel consumption on HC and CO emissions appears to be more than significant than those for the NO_x emissions.

Flight phase duration vs. amount of emissions

The impact is investigated for the flight phase duration on the large emissions seen in certain flight phases. For instance, the flight phase P9 exhibits the highest HC and CO emissions and the highest flight phase duration for the flights in both routes. However, such a relation is not observed between NO_x emissions and fuel consumption. Accordingly, close correlation coefficients for the relationship between the flight phase duration and HC and CO emissions are observed for flights on both routes (the correlation coefficients of HC and CO emissions, respectively, are found to be 0.709 and 0.731 for AYT-SAW and 0.803 and 0.816 for ADB-SAW). The correlation between NO_x emissions and flight phase duration is found to be 0.771 for AYT-SAW and 0.761 for ADB-SAW. As expected, there is no significant relationship between fuel consumption and flight phase.

No significant relationship is found between fuel consumption per flight phase and phase duration. This is an expected result since the time in mode of ground operation of aircraft is greatly affected by the traffic volume of the airport. For instance, the engine can run for a long time in the idle power setting, and due to the low fuel flow rate, the total fuel consumption for this phase would be much lower compared to those for other phases. On the other hand, although short in duration, the total fuel flow rates during takeoff could be 8 to 10 times higher than those for idle, leading to a higher total fuel consumption. The corresponding correlation coefficients are found to be low, at 0.607 and 0.586 for AYT and ADB, respectively.

It is noted that two common methodologies are used to estimate the fuel flow rate of commercial aircraft, namely, the Base of Aircraft Data (BADA) and Boeing Fuel Flow methods. In the BADA method, a total

energy model is used for a wide range of aircraft types which involves all the forces acting on the aircraft and the variations of potential and kinetic energies. In the Boeing method, fuel flow data from the ICAO emission databank, which are calibrated to temperature and pressure ratios to obtain corrected fuel flows for the related cruise altitude and engine power, are used. However, since each method is based on fuel flow estimates considering relatively limited operating conditions, there exists the potential for high levels of error. This study, on the other hand, is believed to generate better estimates since it is based on actual flight data.

Conclusion

For the common emission species CO, HC, and NO_x, linear and nonlinear models are developed in this study for all flight phases, for two routes, and two engine models. The models are based on the ICAO emission measurements. Actual flight data are obtained from flight data records. The models permit evaluation of emissions for all of flight phases for various fuel flow rates.

The models can be used for other aircraft types using the same types of the engines. That is, for the same engine type and known fuel flow rates, emission quantities can be calculated using the developed models. A breakdown of emissions by flight phase is obtained, and the findings agree well for flights on both routes. Accordingly, the highest CO and HC emissions are found in the descent phase followed by the taxi phases (in and out). The highest NO_x emissions are found in the climb phase followed by the cruise and descent phases. There are less but not negligible NO_x emissions in the taxi phase due to the high taxi duration. The mean total flight emissions are calculated as 8 kg of HC, 75 kg of HC, and 31 kg of NO_x for the AYT route and 6 kg of CO, 60 kg of HC, and 28 kg of NO_x for the ADB route. Lastly, the average ground time of the flights are calculated as 22% to 25% of the total flight time for both routes. Since the HC and CO emissions are mostly produced at the lower power settings of the engine, decreasing the taxiing time provides significant abatement of those two emissions.

The authors believe that in order to characterize emissions in a broader sense, future research is merited to perform emission tests in a widespread manner, while the ICAO time in mode assumptions could be updated and better estimations introduced. In the same manner, the ICAO fuel flow assumptions could be revised, and instead of absolute values, certain intervals could be used.

Abbreviations

ADB: Izmir Adnan Menderes International; AYT: Antalya International;
CO: Carbon monoxide; EGT: Exhaust gas temperature; EI: Emission index;
EPA: Environmental Protection Agency; ff: Fuel flow rate (kg/h, kg/s);
HC: Hydrocarbon; ICAO: International Civil Aviation Organization;
LTO: Landing and takeoff; NO_x: Nitrogen oxide; RPM: Revolutions per minute;
R²: Coefficient of determination; SAW: Istanbul Sabiha Gokcen International.

Competing interests

The authors declare that they have no competing interests.

Authors' contributions

ETT and OU carried out the analysis and drafted the manuscript. MAR checked the analysis and reviewed the revised manuscript. All authors read and approved the final manuscript.

Authors' information

ETT is a doctor who is an assistant professor in the Faculty of Aeronautics and Space Sciences at Anadolu University. He received his BSc and MSc in the School of Civil Aviation and Graduate School of Sciences at Anadolu University in 1999 and 2003, respectively. He received his PhD in 2007. OU received her BSc degree in Electrical and Electronics Engineering from Anadolu University in 1990 and her MSc degree in Exploitation Aeronautique from Ecole Nationale de l'Aviation Civile. She received her PhD degree from the Graduate School of Science, Department of Civil Aviation at Anadolu University in 1999 and has been working at the Department of Air Traffic Control, Faculty of Aeronautics and Space Sciences, Anadolu University as an assistant professor. MAR is a professor in the Faculty of Engineering and Applied Science at the University of Ontario Institute of Technology, where he was a founding dean from 2002 to 2008. He was the former president of the Engineering Institute of Canada. He served as president of the Canadian Society for Mechanical Engineering and is a fellow of that society as well as the Engineering Institute of Canada, the Canadian Academy of Engineering, the American Society of Mechanical Engineers, and the International Energy Foundation. Previously, he was the chair of the Department of Mechanical Engineering at Ryerson University.

Acknowledgments

The authors thank Captain Cahit Tasbas, Captain Mustafa Kemal Helvacioğlu, and FDM Specialist Ms. Sercin Ozen from Pegasus Airlines for their co-operation, and the Sabiha Gokcen Airport Authority for its kind assistance in data acquisition. The authors also thank Anadolu University for the financial support.

Author details

¹Department of Airframe and Powerplant Maintenance, Faculty of Aeronautics and Space Sciences, Anadolu University, Eskisehir 26470, Turkey.

²Department of Air Traffic Control, Faculty of Aeronautics and Space Sciences, Anadolu University, Eskisehir 26470, Turkey. ³Faculty of Engineering and Applied Science, University of Ontario Institute of Technology, 2000 Simcoe Street North, Oshawa, Ontario L1H 7K4, Canada.

Received: 29 August 2012 Accepted: 21 March 2013

Published: 3 April 2013

References

1. Baughcum, SL, Tritz, TG, Henderson, SC, Pickett, DC: Scheduled Aircraft Emission Inventories for 1992: Database Development and Analysis. NASA contract report no. 4700. NASA Langley Research Centre, Hampton, VA (1996)
2. Sutkus, DJ, Baughcum, SL, DuBois, DP: Scheduled Civil Aircraft Emission Inventories for 1999: Database Development and Analysis. Report NASA/CR-2001-211216. NASA Center for Aerospace Information, Hanover, MD (2001)
3. Gardner, RM, Adams, K, Cook, T, Deidewig, F, Ernedal, S, Falk, R, Fleuti, E, Herms, E, Johnson, CE, Lecht, M, Lee, DS, Leech, M, Lister, D, Massé, B, Metcalfe, M, Newton, P, Schmitt, A, Vandenbergh, C, Drimmelen, R: The ANCAT/EC global inventory of NO_x emissions from aircraft. *Atmos. Environ.* **31**(12), 1751–1766 (1997)
4. Evers, CJ, Addleton, D, Atkinson, K, Broomhead, MJ, Christou, R, Elliff, T, Falk, R, Gee, I, Lee, DS, Marizy, C, Michot, S, Middel, J, Newton, P, Norman, P, Plohr, M, Raper, D, Stanciou, N: AERO2k Global Aviation Emissions Inventories for 2002 and 2025. European Commission, Contract No. G4RD-CT-2000-00382, QinetiQ Ltd, Farnborough, Hampshire (2004)
5. Kim, BY, Fleming, GG, Balasubramanian, S, Malwitz, A, Lee, J, Ruggiero, J, Klima, K, Lock, M, Holsclaw, CA, Morales, A, McQueen, E, Gillette, W: System for assessing aviation's global emissions (SAGE), version 1.5, global aviation emissions inventories for 2000 through 2004. Report FAA-EE-2005-02, Federal Aviation Administration, Office of Environment and Energy, Washington, DC (2005)

6. U.S. Environmental Protection Agency: Environmental Fact Sheet, Adopted Aircraft Engine Emission Standards, EPA 420-F-97-010. <http://www.epa.gov/oms/regs/nonroad/aviation/aircr-fr.pdf> (1997). Accessed 28 April 2011
7. Schafer, K, Jahn, C, Sturm, P, Lechner, B, Bacher, M: Aircraft emission measurements by remote sensing methodologies at airports. *Atmos. Environ.* **37**(37), 5261–5271 (2003)
8. Herndon, SC, Shorter, JH, Zahniser, MS, Nelson, DD, Jayne, J, Brown, RC, Miake-Lye, RC, Waitz, I, Silva, P, Lanni, T, Demerjian, K, Kolb, CE: NO and NO₂ emission ratios measured from in-use commercial aircraft during taxi and takeoff. *Environ. Sci. Technol.* **38**(22), 6078–6084 (2004)
9. Unal, A, Hu, Y, Chang, ME, Odman, MT, Russell, AG: Airport related emissions and impacts on air quality: application to the Atlanta International Airport. *Atmos. Environ.* **39**(32), 5787–5798 (2005)
10. Herndon, SC, Rogers, T, Dunlea, EJ, Jayne, JT, Miake-Lye, R, Knighton, B: Hydrocarbon emissions from in-use commercial aircraft during airport operations. *Environ. Sci. Technol.* **40**(14), 4406–4413 (2006)
11. Winther, M, Kousgaard, U, Oxbel, A: Calculation of odour emissions from aircraft engines at Copenhagen Airport. *Sci. Total Environ.* **366**(1), 218–232 (2006)
12. Schurmann, G, Schafer, K, Jahn, C, Hoffmann, H, Bauerfeind, M, Fleuti, E, Rappengluck, B: The impact of NO_x, CO and VOC emissions on the air quality of Zurich airport. *Atmos. Environ.* **41**, 103–118 (2007)
13. Westerdahl, D, Fruin, SA, Fine, PL, Sioutas, C: The Los Angeles International Airport as a source of ultrafine particles and other pollutants to nearby communities. *Atmos. Environ.* **42**(13), 3143–3155 (2008)
14. Civil Aviation Authority (CAA): ICAO Emission Databank. <http://easa.europa.eu/environment/edb/docs/edb-emissions-databank.xls> (2013). Accessed 10 April 2013
15. U.S. Department of Transportation, Federal Aviation Administration: CFM56-7B type certification, Type Certificate Data Sheet E00055EN. [http://rgl.faa.gov/Regulatory_and_Guidance_library/rgMakeModel.nsf/0/a25bbd09030a2d0d862574fa00744f01/\\$FILE/E00055EN.pdf](http://rgl.faa.gov/Regulatory_and_Guidance_library/rgMakeModel.nsf/0/a25bbd09030a2d0d862574fa00744f01/$FILE/E00055EN.pdf) (2008). Accessed 28 April 2011
16. Herndon, S: Measurement of Gaseous HAP Emissions from Idling Aircraft as a Function of Engine and Ambient Conditions. Transportation Research Board, Report 63, Washington, USA (2012)
17. Timko, MT, Herndon, SC, Wood, EC, Onasch, TB, Northway, MJ, Jayne, JT, Canagaratna, MR, Miake-Lye, RC, Knighton, WB: Gas turbine engine emissions—part I: volatile organic compounds and nitrogen oxides. *Journal of Engineering for Gas Turbines and Power* **132**, 061504 (2010)
18. Yelvington, PE, Herndon, SC, Wormhoudt, JC, Jayne, JT, Miake-Lye, RC, Knighton, WB, Wey, C: Chemical speciation of hydrocarbon emissions from a commercial aircraft engine. *Journal of Propulsion and Power* **23**(5), 912–918 (2007)
19. Brasseur, GP, Cox, RA, Hauglustaine, D, Isaksen, I, Lelieveld, J, Lister, DH, Sausen, R, Schumann, U, Wahner, A, Wiesen, P: European scientific assessment of the atmospheric effects of aircraft emissions. *Atmos. Environ.* **32**(13), 2329–2418 (1998)
20. Giampaolo, T: *The Gas Turbine Handbook: Principles and Practices*, 2nd edn. Fairmont Press, Lilburn (2003)
21. Hunecke, K: *Jet Engines: Fundamentals of Theory, Design and Operation*, 6th edn. Motorbooks International Publishers, Osceola (2003)
22. Mazaheri, M, Johnson, GR, Morawska, L: Particle and gaseous emissions from commercial aircraft at each stage of the landing and takeoff cycle. *Environ. Sci. Technol.* **43**, 441–446 (2009)
23. Anderson, BE, Chen, G, Blake, DR: Hydrocarbon emissions from a modern commercial airliner. *Atmos. Environ.* **40**, 3601–3612 (2006)

doi:10.1186/2251-6832-4-15

Cite this article as: Turgut *et al.*: Empirical model assessment of commercial aircraft emissions according to flight phases. *International Journal of Energy and Environmental Engineering* 2013 **4**:15.